Published in final edited form as:
Cell Host Microbe. 2015 January 14; 17(1): 47–57. doi:10.1016/j.chom.2014.12.001.

Hepcidin-Induced Hypoferremia Is a Critical Host Defense Mechanism Against the Siderophilic Bacterium *Vibrio vulnificus*

João Arezes[1,2], **Grace Jung**[1], **Victoria Gabayan**[1], **Erika Valore**[1], **Piotr Ruchala**[1], **Paul A. Gulig**[3], **Tomas Ganz**[1,*], **Elizabeta Nemeth**[1,4], and **Yonca Bulut**[1,4]

[1]David Geffen School of Medicine at UCLA, Los Angeles, CA 90095, USA

[2]Graduate Program in Areas of Basic and Applied Biology, Abel Salazar Biomedical Sciences Institute, University of Porto, Porto 4050, Portugal

[3]Department of Molecular Genetics and Microbiology, University of Florida, Gainesville, FL 32601 USA

SUMMARY

Hereditary hemochromatosis, an iron overload disease caused by a deficiency in the iron-regulatory hormone hepcidin, is associated with lethal infections by siderophilic bacteria. To elucidate the mechanisms of this susceptibility, we infected wild-type and hepcidin-deficient mice with the siderophilic bacterium *Vibrio vulnificus*, and found that hepcidin deficiency results in increased bacteremia and decreased survival of infected mice, which can be partially ameliorated by dietary iron depletion. Additionally, timely administration of hepcidin agonists to hepcidin-deficient mice induces hypoferremia that decreases bacterial loads and rescues these mice from death, regardless of initial iron levels. Studies of *Vibrio vulnificus* growth *ex vivo* show that high iron sera from hepcidin-deficient mice support extraordinarily rapid bacterial growth, and that this is inhibited in hypoferremic sera. Our findings demonstrate that hepcidin-mediated hypoferremia is a host defense mechanism against siderophilic pathogens and suggest that hepcidin agonists may improve infection outcomes in patients with hereditary hemochromatosis or thalassemia.

INTRODUCTION

Iron, required as a co-factor for many important biological processes, is an essential nutrient for nearly all living organisms. The requirement for this metal places it in a critical role at the host-pathogen interface: microbes evolved complex means to acquire iron from the host

[*]Correspondence: TGanz@mednet.ucla.edu; phone: 310-825-6112; fax: 310-206-8766.
[4]Contributed equally

AUTHORS CONTRIBUTION

JA and YB designed and performed experiments, analyzed data, and wrote the paper; GJ, VG, and EV performed experiments and analyzed data, PR designed and prepared minihepcidins; PAG developed V. vulnificus strains, contributed to experimental design and wrote the paper; and TG and EN designed experiments, analyzed data and wrote the paper.

(Marx, 2002; Schaible and Kaufmann, 2004) and the host evolved the ability to resist infection by sequestering iron so it is less available to microbes.

Hereditary hemochromatosis, a common genetic iron overload disease (Ganz and Nemeth, 2011), increases susceptibility to infections with *Vibrio vulnificus* and *Yersinia enterocolitica* (Khan et al., 2007), gram-negative bacteria classified as “siderophilic” because their pathogenicity is enhanced by excess iron (Weinberg, 2008, 2009). *Vibrio vulnificus* causes fulminant sepsis with mortality higher than 50% in susceptible patients including those with hereditary hemochromatosis and other iron overload conditions (Horseman and Surani, 2011) but it does not cause severe illness in healthy individuals. It is not known which specific manifestations of hereditary hemochromatosis predispose to infection with siderophilic microbes: liver injury, tissue iron loading, high baseline plasma iron concentrations or the inability to lower iron concentrations in plasma in response to infections.

Hereditary hemochromatosis is caused by deficiency of the iron-regulatory hormone hepcidin (Ganz and Nemeth, 2011). Hepcidin is a 25 amino acid peptide secreted by hepatocytes. It controls iron concentrations in extracellular fluid and blood plasma by regulating the amount of ferroportin, the sole known cellular iron exporter. Ferroportin transports absorbed, recycled or stored iron from tissues into plasma (Donovan et al., 2005). Hepcidin binding to ferroportin triggers its degradation, resulting in decreased transfer of iron to plasma and consequently hypoferremia (Nemeth et al., 2004b). During infections or in response to injection of microbial molecules, hepcidin production is greatly enhanced (Armitage et al., 2011; Rodriguez et al., 2014), stimulated by inflammatory cytokines including IL-6 (Nemeth et al., 2004a; Rodriguez et al., 2014) and possibly activin B (Besson-Fournier et al., 2012). It has been proposed that hepcidin-mediated hypoferremia functions as a host defense mechanism that evolved to restrict iron availability for pathogen growth (Drakesmith and Prentice, 2012; Ganz, 2009) but this has never been demonstrated. Hepcidin was also reported to have direct bactericidal activity *in vitro* (Krause et al., 2000; Park et al., 2001), but the effect is seen only at unphysiologically high concentrations.

Here we demonstrate that hepcidin has a critical role in host defense against *V. vulnificus* by inducing reactive hypoferremia during early phases of infection. In addition, we show that acute pre- or post-exposure treatment of susceptible mice with hepcidin agonists mitigates the high mortality caused by this pathogen.

RESULTS

Hepcidin is required for resistance to *V. vulnificus* infection

Iron is thought to be required for rapid growth of *V. vulnificus* and lethality during infections, as was previously demonstrated in mice injected with iron-dextran (Starks et al., 2000; Wright et al., 1981). To examine whether the iron-regulatory hormone hepcidin affects the response to infection, we compared the severity of the *V. vulnificus* infection in wild-type (WT) and hepcidin knock-out (*Hamp1*$^{-/-}$) mice. Mice were iron-depleted or iron-loaded by dietary manipulations, and infected subcutaneously with a low (10^3 CFU) or moderate (10^5 CFU) inoculum of *V. vulnificus*. In both iron-depleted (Figure 1A) and iron-

loaded (Figure 1B) conditions *Hamp1*$^{-/-}$ mice were significantly more susceptible than WT mice: iron-loaded *Hamp1*$^{-/-}$ died within one day after infection, iron-depleted *Hamp1*$^{-/-}$ within next several days, whereas WT mice survived the infection. WT mice were susceptible to *V. vulnificus* infection only when iron-loaded (Table S1) and infected with a large inoculum of *V. vulnificus* (10^6 CFU). Under those conditions, iron-loaded mice died within 2 days after infection while most of the iron-depleted mice still survived (Figure S1A), confirming that iron has a striking effect on *V. vulnificus* lethality. The differential susceptibility of WT and *Hamp1*$^{-/-}$ to *V. vulnificus* infection was not attributable to their baseline liver iron differences because iron-depleted *Hamp1*$^{-/-}$ mice were much more susceptible to infection even though they had lower liver iron stores than iron-overloaded WT mice, as measured in a parallel set of mice maintained under the same conditions as the mice used for the survival experiments (Figure 1C). As *V. vulnificus* is an extracellular pathogen (Gulig et al., 2005), intracellular hepatocyte iron is not likely to play a direct role in the growth of these bacteria.

To examine whether extracellular iron concentrations alter the growth rate of *V. vulnificus*, we assessed bacterial growth *ex vivo* in sera collected from uninfected iron-loaded or iron-depleted WT animals. *V. vulnificus* growth was greatly enhanced in serum derived from iron-loaded compared to iron-depleted mice (Figure S1B). Supplementing iron-depleted serum with ferric ammonium citrate (FAC) also enhanced bacterial growth. Conversely, addition of the synthetic iron chelator deferiprone to iron-rich serum prevented bacterial growth. Interestingly, growth in low-iron serum was similar to the growth under standard conditions in LB-N broth. This indicates that *V. vulnificus* can grow adequately even with limited iron availability but that excess iron greatly increases the growth rate. In iron-rich serum, bacteria underwent ~18 divisions within 3 hours, or one division every 10 min, an astoundingly rapid growth rate.

Human infections with *V. vulnificus* and their laboratory models often terminate in septic shock (Shan et al., 2012). To verify that this mechanism contributed to rapid death of iron-loaded mice, we inspected H&E stained skin (site of injection) and liver sections of *Hamp1*$^{-/-}$ mice injected with $1x10^3$ CFU of *V. vulnificus* or saline. The venules in the skin and hepatic circulation of infected mice were greatly dilated compared with saline-treated mice (Figure 2A–D and E–H). The vasodilatation was accompanied by erythrocyte sludging characteristic of circulatory shock. In the skin, massive aggregates of bacteria were visible in the perivascular space (Figure 2E–H). In the liver, no bacteria were seen but there was neutrophilic infiltration in perivenular spaces (Figure S2). These findings are consistent with endotoxemic shock.

To determine whether the susceptibility of *Hamp1*$^{-/-}$ mice to severe *V. vulnificus* infection was due to greater bacteremia and bacterial dissemination, we assayed bacterial CFU counts in blood and liver of iron-depleted and iron-loaded WT and *Hamp1*$^{-/-}$ mice 16 h after infection. Liver CFU counts likely represent extracellular bacteria as *V. vulnificus* does not appear to invade cells (Gulig et al., 2005). To allow *Hamp1*$^{-/-}$ mice to survive long enough to undergo analysis at the 16 h time point, we injected all groups with a small inoculum of bacteria (300 CFU). After infection with this low dose, only iron-loaded *Hamp1*$^{-/-}$ mice, but not iron-depleted *Hamp1*$^{-/-}$ or either of the WT groups, had CFU in blood and liver

(Figure 3A). For the WT groups, the iron-dependent difference in CFUs was observed at a higher inoculum (10^5 CFU, Figure 3B). These data indicate that in both *Hamp1*$^{-/-}$ and WT mice, bacterial replication and dissemination is highly dependent on the host's iron status. As shown in Figure 1, mortality from *V. vulnificus* infection did not correlate with baseline liver iron concentrations, therefore we hypothesized that the difference in baseline serum iron concentrations, baseline non-transferrin bound iron (NTBI) and/or the ability to generate hypoferremia may explain the disparate susceptibility of *Hamp1*$^{-/-}$ and WT mice and the iron dependence of bacterial growth *in vivo*. Indeed, WT mice lowered their serum iron concentrations in response to infection (Figure 3C, mean of 26 μM in iron-depleted and 30 μM in iron-loaded infected mice), whereas *Hamp1*$^{-/-}$ mice had a much smaller decrease in serum iron (mean of 63 μM in iron-depleted and 52 μM in iron-loaded infected mice), insufficient to affect the replication of *V. vulnificus*. The slight decrease in *Hamp1*$^{-/-}$ serum iron may be a consequence of decreased food intake, a common trait in sick mice, or due to direct effects of inflammatory cytokines on ferroportin mRNA (Ludwiczek et al., 2003).

Among *Hamp1*$^{-/-}$ mice, despite similar serum iron concentrations in iron-loaded and iron-depleted groups, the iron-loaded group had higher CFU counts in the blood and liver (Figure 3A). This difference in bacterial burden may be related to the difference in the serum concentrations of NTBI, a known source of iron for *V. vulnificus* (Kim et al., 2007). NTBI was only detected in iron-loaded mice (1.28± 0.60 LPI units), but not in the iron-depleted group (Figure 3D), correlating with the bacterial burden. WT mice had low NTBI levels, similar to those in iron-depleted *Hamp1*$^{-/-}$ mice, suggesting that NTBI did not contribute to bacterial growth in WT mice. Among WT mice infected with the high inoculum (10^5 CFU), the iron-loaded group had higher CFU counts in the blood and liver than the iron-depleted group (Figure 3B), despite the similar degree of hypoferremia 16 h after infection (Figure 3C). As NTBI levels were not significantly different between these two groups, it is likely that serum iron concentrations during the early stages of infection (prior to the hepcidin increase and hypoferremia) also contribute to susceptibility to *V. vulnificus* infection. Thus, our data suggest that baseline concentrations of transferrin-bound and non-transferrin bound iron as well as reactive hypoferremia, all of which are controlled by hepcidin, determine the replication and dissemination of *V. vulnificus* in vivo.

Hepcidin levels increase early after *V. vulnificus* infection

Only WT but not *Hamp1*$^{-/-}$ animals were able to generate significant hypoferremia, suggesting that hepcidin mediates inflammatory hypoferremia during infection. To confirm this hypothesis we analyzed hepatic hepcidin mRNA and serum hepcidin protein at 3, 6 and 10 hours after infection with 10^5 *V. vulnificus* in iron-loaded and iron-depleted WT mice. As expected, iron-loaded mice had higher levels of hepcidin mRNA and protein compared to iron-depleted mice at all time points (Figure 4A,B). By 6 h after infection, both iron-depleted and iron-loaded mice acutely increased their hepatic hepcidin mRNA (Figure 4A) as well as serum hepcidin concentration (Figure 4B) compared to uninfected mice. At 10 h after infection, serum hepcidin increased further in iron-depleted mice and stabilized at very high levels in iron-loaded mice (Figure 4B). These increases in hepcidin concentrations were accompanied by a significant decrease in serum iron at 6 h and 10 h in iron-depleted mice (Figure 4C), and a trend toward decreased serum iron in iron-loaded mice. The latter may

not have decreased serum iron as efficiently because iron–loaded hepatocytes, macrophages and enterocytes express more ferroportin (Chua et al., 2006; Delaby et al., 2005; Zoller et al., 2002).

IL-6 is thought to be the predominant stimulus for hepcidin synthesis during inflammation (Nemeth et al., 2004a; Rodriguez et al., 2014). We found dramatically increased serum concentrations of this pro-inflammatory cytokine in infected mice starting at 3 h after infection (Figure 4D), with no differences between iron-depleted and iron-loaded mice. A similar increase was also observed for the inflammatory cytokines KC-GRO, IL-12p70, IL-1β, TNF-α, IL-10 and IL-2, while IFN-γ, IL-4 and IL-5 remained unchanged (Figure S4C). We also observed early increases in hepatic *Saa1* and *Inhbb* mRNA (Figure S4A and B).

Interestingly, at 16h after infection, no statistically significant differences in hepcidin were observed between infected and saline-treated WT mice, either at the hepatic mRNA or serum protein levels (Figure S3A,B), despite increased inflammatory markers, including hepatic *Saa1* mRNA (Figure S3C) and pro-inflammatory cytokines in the serum (Figure S3E). *Inhbb* mRNA, coding for the β_B-subunit of activin B, a protein involved in an alternative pathway for hepcidin regulation by inflammation, was also increased in infected iron-loaded groups (Figure S3D). These data imply that hepcidin production in the liver was rapidly increased early in the course of infection by inflammatory mediators induced by bacterial infection. Elevated hepcidin in turn caused acute hypoferremia. The hypoferremia appears to counterregulate hepcidin so that by 16 h hepcidin levels in infected WT mice were no longer different from uninfected controls.

Minihepcidin PR73 protects against mortality from infections with *Vibrio vulnificus*

To further examine the importance of early hepcidin activity for resistance to *V. vulnificus* infection, we tested the therapeutic effect of minihepcidin PR73 (a synthetic hepcidin agonist, Figure S5) in *Hamp1*$^{-/-}$ mice. We used minihepcidin because it has greater potency and longer lasting effect than full-length hepcidin (Ramos et al., 2012). Mice were pretreated with PR73 24h and 3h before infection and were euthanized 16h after s.c. infection with 300 CFU of *V. vulnificus*. Administration of minihepcidin caused marked hypoferremia (3 μM in iron-depleted and 9 μM in iron-loaded mice) (Figure 5A). Liver iron stores did not change likely because of the short duration of the experiment (40 h) (Figure 5B). Importantly, minihepcidin treatment resulted in decreased numbers of bacteria in blood and liver of both iron-depleted and iron-loaded mice (Figure 5C,D). Pretreatment with PR73 also markedly improved survival: while most of the non-treated *Hamp1*$^{-/-}$ mice died within 2 days after infection with 10^3 or 10^5 CFU of *V. vulnificus*, mice treated with minihepcidin survived, regardless of their iron load and regardless of the number of bacteria administered (Figure 6A,B).

To test whether minihepcidins are effective not only for the prevention but also post-exposure treatment of *V. vulnificus* infection, we injected PR73 in iron-loaded *Hamp1*$^{-/-}$ mice 3 h after infection with 10^3 CFU of bacteria. Even delayed injection (post exposure treatment) of PR73 significantly increased the survival of these highly susceptible mice (Figure 6C).

To determine if the anti-Vibrio effect of minihepcidin was due to iron restriction of bacterial growth or a direct bactericidal effect of the PR73 peptide, we measured the growth and killing of a *V. vulnificus* strain marked by a chloramphenicol-resistance plasmid, similarly to a published approach (Figure S7) (Gulig et al., 1997). The marker plasmid only replicates in the presence of arabinose, which is not present in significant amounts in mouse serum. Bacteria were grown *ex vivo* in sera that were obtained from *Hamp1*$^{-/-}$ mice treated with PR73 minihepcidin or with a solvent control. Iron concentrations of these sera are provided in Table S2. After incubating bacteria in the mouse sera for 2 h, CFU counts were determined on plates that allow only plasmid-containing bacteria to grow (supplemented with chloramphenicol and arabinose) or plates that allow all Vibrio bacteria to grow (no chloramphenicol/arabinose). Because the marker plasmid does not replicate in bacteria growing in serum, the reduction in CFU of plasmid-containing Vibrio reflects the killing of the inoculum. The number of total Vibrio CFU reflects both growth and killing of bacteria whereas the ratio of total to plasmid-containing bacteria (T/P) reflects growth only (Gulig et al., 1997) (Figure S7).

After incubation in *ex vivo* sera, total CFU were 15–20-fold lower in sera of minihepcidin-treated *Hamp1*$^{-/-}$ mice compared to the sera of solvent-treated *Hamp1*$^{-/-}$ mice (Figure 7A), regardless whether the donor mice were on low or high iron diet, mirroring the *in vivo* CFU results (Figure 5C,D). In contrast, CFU of the plasmid-containing bacteria were merely 1.7–1.9-fold lower in minihepcidin-treated sera relative to the solvent sera (Figure 7B), demonstrating that the peptide had only a slight bactericidal effect in serum. T/P ratios (i.e. bacterial growth) were about ten-fold lower for sera from the minihepcidin-treated mice compared with the solvent controls (Table S2), indicating that minihepcidin-triggered hypoferremia significantly decreased bacterial replication. This effect of hypoferremia on Vibrio growth was also replicated using sera from noninfected WT mice that were fed low- or high-iron diet (Figure 7C,D). Moderately hypoferremic sera (because of low-iron diet) slowed down Vibrio growth compared to iron-rich sera (because of high-iron diet), as shown by a more than 10-fold decreased T/P ratio (Table S2), without affecting the number of plasmid-containing bacteria (Figure 7D). Thus, minihepcidin-induced hypoferremia rather than a direct antimicrobial effect of minihepcidin was responsible for slower Vibrio replication.

Like healthy humans, WT mice, which appropriately respond to infection by inducing endogenous hepcidin, are highly resistant to *V. vulnificus* infection. When very large inocula of *V. vulnificus* (10^6 and 10^7 CFU) were administered to WT mice, minihepcidins did not further protect them from lethal infection (Figure S6), arguing against a direct microbicidal effect of these peptides *in vivo*.

DISCUSSION

The growth of pathogens in their hosts is critically dependent on the pathogens' ability to capture and utilize iron. The hosts have evolved several countermeasures to restrict the bioavailability of iron and effectively starve the microbes (Ganz, 2009). Hepcidin-induced hypoferremia has been proposed as an important host defense mechanism (Drakesmith and Prentice, 2012; Ganz, 2009), but specific support for its role has been lacking. In this study,

we show that acute hypoferremia is an important host defense mechanism against the siderophilic bacterial pathogen *V. vulnificus*.

After infection with *V. vulnificus*, iron-loaded mice had greater bacterial CFU burden in blood and the liver. Moreover, *ex vivo* sera that had excess iron promoted the rapid growth of *V. vulnificus*. This is not a result of the inability of these bacteria to utilize iron at its physiologic concentration because bacteria grew well even in sera with relatively low iron levels. Rather, high iron levels trigger extraordinarily rapid *V. vulnificus* growth, with bacteria dividing every 10 min. We speculate that high iron concentrations, or possibly the related presence of one or more non-transferrin bound iron (NTBI) forms in the environment of *V. vulnificus*, activate a genetic program for very rapid growth, leading to septicemia, high cytokine concentrations, evidence of septic shock at necropsy and early mortality. The early mortality of susceptible humans after infection with these bacteria suggests that a similar program may be activated during human infections with *V. vulnificus*.

In our mouse models, the order of susceptibility to rapid mortality from *V. vulnificus* was *Hamp1*$^{-/-}$ iron-overloaded > *Hamp1*$^{-/-}$ iron-depleted > WT iron-overloaded > WT iron-depleted. This together with studies of the effect of serum iron on *V. vulnificus* growth ex vivo indicated that plasma iron concentrations during the course of infection determined the growth of *V. vulnificus* and host mortality. *Hamp1*$^{-/-}$ mice were more susceptible to lethal infection, even when they had the same baseline serum iron and lower liver iron stores than iron loaded WT mice. This suggests that acute hypoferremia after infection is a major iron-related determinant of resistance to *V. vulnificus*.

WT mice developed hypoferremia within hours after infection with *V. vulnificus*, and this response was dependent on early induction of hepcidin, preceded by a rise in inflammatory cytokines such as IL-6 and activin B. IL-6 acts as an inflammatory signal that triggers hepcidin expression in the liver through the JAK/STAT3 pathway (Nemeth et al., 2004a; Verga Falzacappa et al., 2007; Wrighting and Andrews, 2006). Activin B, through SMAD1/5/8 signaling (Besson-Fournier et al., 2012), is also a stimulus for hepcidin production in response to inflammation. We found that expression of *Inhbb*, encoding the activin β_B-subunit, is increased prior to the hepcidin response, suggesting that the two pathways may cooperate in the induction of hepcidin during infection.

To further examine if hepcidin-induced hypoferremia is an effective component in the innate immune response against *V. vulnificus*, we analyzed the therapeutic effects of minihepcidins in *Hamp1*$^{-/-}$ mice. Minihepcidins are synthetic hepcidin agonists previously shown to bind ferroportin and induce its endocytosis and proteolysis, thus preventing iron overload in hepcidin-deficient mice (Preza et al., 2011; Ramos et al., 2012). In the current study, the short-term minihepcidin treatment robustly decreased serum iron without altering liver iron stores. Both pretreatment with minihepcidin and administration 3h after the infection protected the highly susceptible *Hamp1*$^{-/-}$ mice from dying from infection, even with a large inoculum of *V. vulnificus*. Minihepcidin-treated mice had much lower concentrations of bacterial CFU in the blood and liver, presumably because of a lower bacterial growth rate due to decreased plasma iron. WT mice with their intact endogenous hepcidin response to infection were not further protected by minihepcidins injections. This limitation is not

clinically important because healthy humans do not develop severe *V. vulnificus* infections. Another study (Pan et al., 2012) showed that treatment with tilapia hepcidin TH(2–3) did increase survival rate in Balb/C mice infected with *V. vulnificus*, and that TH(2–3) had both antimicrobial and immunomodulatory effects. However, effects on iron metabolism were not investigated and it is not known if TH(2–3) interacts with murine ferroportin.

Since hepcidin and its fragments have microbicidal effects *in vitro* (Park et al., 2001), we tested if the minihepcidin had a bactericidal effect on *V. vulnificus*. By using a *V. vulnificus* strain containing a marker plasmid, pGTR905, that functions as a replicon only in the presence of arabinose (a sugar not found in relevant concentrations in animal tissues), we demonstrated that the minihepcidin-containing serum had only a slight bactericidal effect that was not sufficient to explain the dramatically lower number of total bacterial CFU. Rather, the slower growth of bacteria in sera from minihepcidin-treated mice was caused by the low iron concentrations in those sera. The dependence of *V. vulnificus* growth in *ex vivo* sera on the serum iron concentrations was confirmed in WT mice where serum iron was manipulated not by the administration of minihepcidin but by changing the dietary iron content. The composition of sera is also not favorable for the direct microbicidal activity of hepcidin which is dependent on acidic pH that is not physiologic in serum (Maisetta et al., 2010).

We cannot exclude the possibility that immunological differences exist between *Hamp1*$^{-/-}$ and WT mice, even when *Hamp1*$^{-/-}$ mice are kept on a low iron diet. Hepcidin deficiency results in altered tissue iron distribution and iron-depleted macrophages, and this could potentially affect innate immune signaling (Oexle et al., 2003; Wang et al., 2009). However, the ability of minihepcidins to rapidly alleviate the mortality of *Hamp1*$^{-/-}$ mice from *V. vulnificus* infection would argue that any immunological differences between *Hamp1*$^{-/-}$ and WT mice are minor or acutely reversible by hepcidin or its analogs. A recent study showed that genes encoding proteins involved in *V. vulnificus* iron acquisition (siderophore receptor *vuuA* and components of siderophore synthase) were induced in bacteria collected from infected patients (Bisharat et al., 2013). Deletion of the *vuuA* gene, which impaired iron uptake from both transferrin and siderophore vulnibactin, resulted in reduced virulence in mice (Webster and Litwin, 2000). However, despite the evident link between the iron uptake and virulence of *V. vulnificus*, the molecular mechanism by which excess iron reprograms *V. vulnificus* for very rapid growth is still elusive.

Human hereditary hemochromatosis is a well-established risk factor for lethal infection with *V. vulnificus*. However, the severity of hepcidin deficiency and iron overload in humans is highly variable, particularly in the most common form caused by the C282Y HFE mutations (Waalen et al., 2002). The variability is attributable to both genetic modifiers (e.g. gender) and environmental factors (e.g. alcohol intake). Therefore, patients with mild or normal phenotypes, will likely not be at increased risk of siderophilic infections. Indeed, studies in HFE knockout mice showed appropriate decrease in serum iron in response to LPS (Wallace et al., 2011). Only when a second hemochromatosis gene TfR2 is ablated is the hypoferremic response to LPS lost (Wallace et al., 2011). Like the HFE mouse model, in the absence of additional genetic or comorbid factors, most patients with HFE mutations may appropriately respond to infections by increasing hepcidin and developing hypoferremia. In

contrast, the loss of hepcidin in *Hamp1*$^{-/-}$ mice generates a particularly severe form of the disease and it nearly completely ablates the hypoferremia of infection. We hypothesize that those hemochromatosis patients with very low baseline hepcidin and impaired hepcidin response to infection, either because of the pattern of causative mutations and/or the presence of comorbid factors, will have increased susceptibility to infections with siderophilic bacteria.

Hepcidin deficiency in humans, such as in fully penetrant forms of hereditary hemochromatosis, is associated with the appearance of NTBI in plasma (Brissot et al., 2012). NTBI was shown to promote the growth of *V. vulnificus* in cirrhotic ascites (Kim et al., 2007) even better than holotransferrin. Our results also demonstrate that the growth of *V. vulnificus in vivo* was highly enhanced in sera containing NTBI. One effect of therapeutically-induced hypoferremia in iron overload would be the loss of NTBI from blood plasma. Further studies are required to elucidate the requirement of NTBI for Vibrio growth in serum and *in vivo*, and its potential mechanisms.

In summary, hepcidin plays an important role in host defense against siderophilic bacteria such as *V. vulnificus* by controlling baseline plasma iron concentrations and mediating hypoferremia in response to infection. These effects prevent the rapid growth of *V. vulnificus* so that other innate immune mechanisms are sufficient to control the infection. Pointing to potential therapeutic applications, pre- or post-infection administration of hepcidin agonists to hepcidin-deficient mice increased their resistance to *V. vulnificus* infection and protected them from consequent mortality.

EXPERIMENTAL PROCEDURES

Preparation of bacteria

Vibrio vulnificus CMCP6 strain was grown in Luria-Bertani broth (Becton Dickinson) containing 0.85% NaCl (LB-N), and bacterial stocks were stored at −80°C in LB-N with 35% glycerol. The day before the experiment, 50 μl of *V. vulnificus* was diluted 1:1000 in LB-N and grown at room temperature overnight. On the day of infection, the culture was diluted 1:30 in LB-N and shaken at 37 °C until the optical density at 600nm reached 0.3. Bacteria were then harvested by centrifugation (13800g for 10 min at 4 °C) and suspended in 0.9% sodium chloride injection solution (Hospira) at the required concentrations. Bacterial CFU were counted by plating 6 μl of serial dilutions of blood, homogenized liver or bacterial suspension on LB-N plates containing 1.5% agar and enumerating the bacterial colonies after incubation at 37°C.

Animal studies

All experiments involving animals were approved by the University of California, Los Angeles (UCLA) Office of Animal Research Oversight. C57BL/6 wild-type mice were obtained from Charles River Laboratories. Hepcidin-1 knockout (*Hamp1*$^{-/-}$) mice (originally provided by Dr. Sophie Vaulont (Lesbordes-Brion et al., 2006) and backcrossed by us onto the C57BL/6 background using marker—assisted accelerated backcrossing (Ramos et al., 2012)) were bred in our vivaria. Only male mice were used. WT and

Hamp1$^{-/-}$ mice were iron-depleted or iron-loaded using dietary manipulations. Starting at 6 weeks of age, WT mice were fed an iron-poor (4 ppm Fe) or iron-rich (10000 ppm Fe) diet (Harlan) for 2 weeks. Starting at 4–5 weeks of age, *Hamp1*$^{-/-}$ mice were fed an iron-poor (4 ppm Fe) or standard diet (270 ppm Fe) for 4–6 weeks before the infection. The earlier start and longer regime of low-iron diet in *Hamp1*$^{-/-}$ was necessary to achieve substantial iron depletion because these mice are already iron-overloaded at a young age.

For survival experiments, animals were infected by subcutaneous (s.c.) injection (100 μl) in the interscapular area with $1x10^3$–$1x10^7$ CFU of *V. vulnificus* suspended in 0.9% sodium chloride (Hospira). Control mice received equivalent injections of saline only. Mice were observed for 4 days or were euthanized earlier by isofluorane (Clipper) inhalation if they became moribund.

For tissue and blood collection, WT and *Hamp1*$^{-/-}$ were infected with 300 CFU (and $1x10^5$ only in WT mice) and control animals received saline-only injections. Mice were euthanized 16–18h after infection, were exsanguinated, and their livers were harvested. For histhopathology analysis, *Hamp1*$^{-/-}$ mice were injected with $1x10^3$ CFU of *V. vulnificus* or saline, euthanized 10–12h after infection and a piece of the liver and the injection site (skin) were collected into tubes containing 4% formalin.

To analyze early changes in iron, hepcidin and pro-inflammatory cytokines after infection, WT mice (fed an iron-poor or iron-rich diet for 2 weeks) were injected with $1x10^5$ CFU of *V. vulnificus* or saline and animals were euthanized at 3, 6 or 10 h after infection.

To test the therapeutic effects of minihepcidin, mice were injected intraperitoneally with 100 nmol of minihepcidin PR73 dissolved in 100 μl of SL220 (Preza et al., 2011; Ramos et al., 2012) (a PEG-phospholipid based solubilizer, NOF Corp.), whereas control groups were injected with the same amount of solvent. For minihepcidin pretreatment studies, animals were injected 24h and 3h before infection. For treatment studies, animals received minihepcidin or solvent injection 3h after the infection. In both experiments, surviving animals also received minihepcidin or solvent injection, 24 and 48 h after infection.

Peptide synthesis

Minihepcidin PR73 was synthesized as a C-terminal amide using standard solid-phase Fmoc chemistry and was purified by preparative reverse-phase high performance liquid chromatography (RP-HPLC). Its purity was evaluated by matrix-assisted laser desorption ionization spectrometry (MALDI-MS) as well as analytical RP-HPLC. From N- to C-terminus the primary sequence of PR73 was: iminodiacetic acid, L-threonine, L-histidine, L-3,3-diphenylalanine, L-β-homoproline, L-arginine, L-cysteine, L-arginine, L-β-homophenylalanine, 6-aminohexanoic acid, iminodiacetic acid palmitylamide (Ida-Thr-His-Dpa-bhPro-Arg-Cys-Arg-bhPhe-Ahx-Ida(NHPal)-CONH2).

Serum and liver iron measurements

Blood was collected in serum separator tubes (BD) and allowed to clot at room temperature for 30 min followed by centrifugation for 5 min, 4500 rpm at 4 C. The serum was transferred to new tubes for serum iron quantification using the colorimetric Iron-SL assay

(Sekisui Diagnostics) following the manufacturer's instructions. For liver iron measurements, the tissue was homogenized and a 75 µl sample was added to 1125 µl of protein precipitation solution (0.53M HCl and 5.3% trichloroacetic acid, Fisher Scientific). The samples were heated at 100 °C for 1 hour, centrifuged for 10 minutes (13000 rpm at 4°C), and the supernatant was used for the Iron-SL assay, measuring the absorbance at 595 nm relative to Iron AA Standard (Ricca Chemical Company). Results are expressed as µg Fe per gram of wet liver weight.

Histopathology analysis

Liver and skin sections were fixed in 4% formalin for 12h, imbedded in paraffin, cut in 5-micron sections and stained with hematoxylin and eosin at the UCLA Translational Pathology Core Laboratory. Skin sections were also stained using the Gram Stain for Tissue kit (Sigma) following the manufacturer's instructions. Microscopic images were acquired on a Nikon Eclipse E600 microscope using Nikon Plan Fluor 4x/0.13, Plan Apo 10×/0.45, Plan Apo 40×/0.95 and Plan Fluor 100x/1.30 objectives with a Spot RT3 2MP Slider camera and Spot 5.0 software. Pictures were assembled using Adobe Photoshop CS5.

Labile plasma iron quantification

Labile plasma iron (LPI), a redox-active form of non-transferrin bound iron(Esposito et al., 2003), was measured using the FeROS eLPI kit (aFerrix) according to the manufacturer's instruction. Briefly, 20 µl of mouse serum was plated in duplicate in 96-well plates. Serum was treated with 100 µl of LPI reagent containing buffered 2,3-dihydrorhodamine and ascorbate, in the presence or absence of an iron chelator. Fluorescence resulting from oxidation of 2,3-dihydrorhodamine after exposure to reactive oxygen species was measured in a Gemini XS microplate reader (Molecular Devices) using 495 nm for excitation and 525 for emission. A kinetic measurement was performed every 2 minutes for 40 minutes. The ΔFU/min for each sample, with or without the iron chelator, was converted to LPI units by comparing it with the standard values obtained in the same test. Values higher than 0.2 were considered indicative for the presence of NTBI.

Gene expression analysis

RNA from mouse liver was extracted by TRIzol Reagent (life technologies), and cDNA was synthesized using the iScript cDNA Synthesis Kit (Bio-Rad) following manufacturer's instructions. Real-time quantification of transcripts was performed in duplicates in a CFX96 Touch Real-Time PCR Detection System (Bio-Rad) using Sso Advance SYBR Green Supermix (Bio-Rad) and specific primers for *Hamp1* (fwd: TTGCGATACCAATGCAGAAGA; rev: GATGTGGCTCTAGGCTATGTT), *Inhbb* (fwd: CTCCGAGATCAT CAGCTTTGC, rev: GGAGCAGTTTCAGGTACAGCC), *Saa1* (fwd: AGTCTGGGCTGCTGAGAAAA; rev: ATGTCTGTTGGCTTCCTGTG) and *Actb* (fwd: ACCCACACTGTGCCCATCTA; rev: CACGCTCGGTCAGGATCTTC). Data were normalized to the expression of β-actin.

Serum hepcidin assay

Mouse hepcidin ELISA was performed as previously described (Kim et al., 2014). Mouse hepcidin-1 monoclonal antibodies, Ab2B10 (capture) and AB2H4-HRP (detection), as well as synthetic mouse hepcidin-25, were a generous gift from Amgen. High binding 96-well EIA plates (Corning Costar) were coated overnight at room temperature with 50 µl/well of 3.6 µg/ml Ab2B10 in 0.2 M carbonate-bicarbonate buffer pH 9.4 (Pierce - Thermo Scientific). Plates were washed two times with wash buffer (PBS, 0.5% Tween-20) and then blocked for 45 minutes with 200 µl/well blocking buffer (PBS, 1% BSA, 1% goat serum, 0.5% Tween-20). Serum samples (previously diluted in blocking buffer at 1:10000 for iron-loaded mice or 1:1000 for iron-depleted mice) and standards were incubated for one hour at room temperature (50 µl/well), washed four times with wash buffer, incubated for one hour with 50 µl/well of 130 ng/ml Ab2H4-HRP, washed 4 times and then developed with 100 µl/well Ultra-TMB substrate (Thermo Scientific) for 15 min in the dark at room temperature. The reaction was stopped by adding 50 µl 2M sulfuric acid, and the absorbance was measured at 450 nm using a 96-well plate reader (Molecular Devices).

Analysis of the bactericidal and bacteriostatic effects of minihepcidin on *V. vulnificus*

To analyze the mode of action of minihepcidin PR73, we used *V. vulnificus* CMCP6 containing pGTR905, a marker plasmid that confers resistance to chloramphenicol, as described in Starks *et al* (Starks et al., 2006). The plasmid replicates only in the presence of arabinose, which is not found in mouse tissues. Thus, the loss of plasmid from the bacterial population during growth in mouse serum is a measure of bactericidal activity. The principle is graphically illustrated in Gulig *et al* (Gulig et al., 1997).

The plasmid-containing bacterial inoculum was first grown in LB-NAC, LB-N broth supplemented with 1% L-arabinose (Sigma) and 5 µg/ml chloramphenicol (Sigma), to enable and select for plasmid replication. The bacteria were then washed, suspended in LB-N at $1x10^5$ CFU/ml and 10 µl added to 40 µl of mouse serum in 96-well plates. Serial 5-fold dilutions were performed in serum. Serum samples were obtained from *Hamp1*$^{-/-}$ mice kept on an iron-poor or standard diet for 4–6 weeks and injected 24 h and 3 h before blood collection with 100 nmoles PR73 in SL220 or with SL220 only (5 mice per group). Sera were also collected from WT mice kept on iron-poor or iron-rich diet for 2 weeks (5 mice per group). For each mouse group, sera was pooled and used for *in vitro* experiments. 96-well plates with bacteria were incubated for 2 h at 37 C with shaking (300 rpm), using triplicates for each condition. Five µl from each well was plated on LB-N and LB-NAC plates (containing 1.5% agar) and CFU were counted for each plate.

Quantification of inflammatory cytokines in serum

Inflammatory cytokines (IFN-γ, IL-1β, IL-2, IL-4, IL-5, IL-6, KC/GRO, IL-10, IL-12p70 and TNF-α) were measured in mouse serum using the Proinflammatory Panel 1 (mouse) kit (Meso Scale Discovery) following manufacturer's instructions. Briefly, 50 µl of standards and 2-fold diluted samples were added to a 10-spot multiplex plate pre-coated with capture antibodies, and the plate was incubated at room temperature with shaking for 2 hours. After washing 3 times with wash buffer (PBS supplemented with 0.05% Tween-20), 25 µl of detection antibody was added to each well and incubated for 2 hours, washed 3 times and

incubated with 150 μl of 2X read buffer (provided with the kit). The plate was read in a chemiluminescence reader (SECTOR Imager 2400, Meso Scale Discovery), and data were analyzed using the MSD Discovery workbench software (Meso Scale Discovery).

Statistical analysis

The statistical significance of differences between groups was evaluated using Student *t* test if data were normally distributed or Mann-Whitney *U* test if this condition was not met. Survival differences were analyzed using Kaplan-Meier survival curves and Log-Rank test. All statistics were done using Sigmaplot 12.5 (Systat Software).

Supplementary Material

Refer to Web version on PubMed Central for supplementary material.

Acknowledgments

We acknowledge The UCLA Translational Pathology Core Laboratory for the assistance with the preparation of the slides for histopathology analysis. This work was supported by UCLA Today's and Tomorrow's Children Fund (to YB), the UCLA Stein/Oppenheimer Endowment Award (to YB), the UCLA Children's Discovery and Innovation Institute and NIH Grant R01 DK090554 (to EN and TG). JA is recipient of a FCT fellowship (www.fct.pt).

References

Armitage AE, Eddowes LA, Gileadi U, Cole S, Spottiswoode N, Selvakumar TA, Ho LP, Townsend AR, Drakesmith H. Hepcidin regulation by innate immune and infectious stimuli. Blood. 2011; 118:4129–4139. [PubMed: 21873546]

Besson-Fournier C, Latour C, Kautz L, Bertrand J, Ganz T, Roth MP, Coppin H. Induction of activin B by inflammatory stimuli up-regulates expression of the iron-regulatory peptide hepcidin through Smad1/5/8 signaling. Blood. 2012; 120:431–439. [PubMed: 22611157]

Bisharat N, Bronstein M, Korner M, Schnitzer T, Koton Y. Transcriptome profiling analysis of Vibrio vulnificus during human infection. Microbiology. 2013; 159:1878–1887. [PubMed: 23782800]

Brissot P, Ropert M, Le Lan C, Loreal O. Non-transferrin bound iron: a key role in iron overload and iron toxicity. Biochimica et biophysica acta. 2012; 1820:403–410. [PubMed: 21855608]

Chua AC, Drake SF, Herbison CE, Olynyk JK, Leedman PJ, Trinder D. Limited iron export by hepatocytes contributes to hepatic iron-loading in the Hfe knockout mouse. Journal of hepatology. 2006; 44:176–182. [PubMed: 16271796]

Delaby C, Pilard N, Goncalves AS, Beaumont C, Canonne-Hergaux F. Presence of the iron exporter ferroportin at the plasma membrane of macrophages is enhanced by iron loading and down-regulated by hepcidin. Blood. 2005; 106:3979–3984. [PubMed: 16081696]

Donovan A, Lima CA, Pinkus JL, Pinkus GS, Zon LI, Robine S, Andrews NC. The iron exporter ferroportin/Slc40a1 is essential for iron homeostasis. Cell metabolism. 2005; 1:191–200. [PubMed: 16054062]

Drakesmith H, Prentice AM. Hepcidin and the iron-infection axis. Science. 2012; 338:768–772. [PubMed: 23139325]

Esposito BP, Breuer W, Sirankapracha P, Pootrakul P, Hershko C, Cabantchik ZI. Labile plasma iron in iron overload: redox activity and susceptibility to chelation. Blood. 2003; 102:2670–2677. [PubMed: 12805056]

Ganz T. Iron in innate immunity: starve the invaders. Current opinion in immunology. 2009; 21:63–67. [PubMed: 19231148]

Ganz T, Nemeth E. Hepcidin and disorders of iron metabolism. Annual review of medicine. 2011; 62:347–360.

Gulig PA, Bourdage KL, Starks AM. Molecular Pathogenesis of Vibrio vulnificus. Journal of microbiology. 2005; 43(Spec No):118–131.

Gulig PA, Doyle TJ, Clare-Salzler MJ, Maiese RL, Matsui H. Systemic infection of mice by wild-type but not Spv- Salmonella typhimurium is enhanced by neutralization of gamma interferon and tumor necrosis factor alpha. Infection and immunity. 1997; 65:5191–5197. [PubMed: 9393815]

Horseman MA, Surani S. A comprehensive review of Vibrio vulnificus: an important cause of severe sepsis and skin and soft-tissue infection. International journal of infectious diseases: IJID: official publication of the International Society for Infectious Diseases. 2011; 15:e157–166. [PubMed: 21177133]

Khan FA, Fisher MA, Khakoo RA. Association of hemochromatosis with infectious diseases: expanding spectrum. International journal of infectious diseases: IJID: official publication of the International Society for Infectious Diseases. 2007; 11:482–487. [PubMed: 17600748]

Kim A, Fung E, Parikh SG, Valore EV, Gabayan V, Nemeth E, Ganz T. A mouse model of anemia of inflammation: complex pathogenesis with partial dependence on hepcidin. Blood. 2014; 123:1129–1136. [PubMed: 24357728]

Kim CM, Park RY, Choi MH, Sun HY, Shin SH. Ferrophilic characteristics of Vibrio vulnificus and potential usefulness of iron chelation therapy. The Journal of infectious diseases. 2007; 195:90–98. [PubMed: 17152012]

Krause A, Neitz S, Magert HJ, Schulz A, Forssmann WG, Schulz-Knappe P, Adermann K. LEAP-1, a novel highly disulfide-bonded human peptide, exhibits antimicrobial activity. FEBS letters. 2000; 480:147–150. [PubMed: 11034317]

Lesbordes-Brion JC, Viatte L, Bennoun M, Lou DQ, Ramey G, Houbron C, Hamard G, Kahn A, Vaulont S. Targeted disruption of the hepcidin 1 gene results in severe hemochromatosis. Blood. 2006; 108:1402–1405. [PubMed: 16574947]

Ludwiczek S, Aigner E, Theurl I, Weiss G. Cytokine-mediated regulation of iron transport in human monocytic cells. Blood. 2003; 101:4148–4154. [PubMed: 12522003]

Maisetta G, Petruzzelli R, Brancatisano FL, Esin S, Vitali A, Campa M, Batoni G. Antimicrobial activity of human hepcidin 20 and 25 against clinically relevant bacterial strains: effect of copper and acidic pH. Peptides. 2010; 31:1995–2002. [PubMed: 20713108]

Marx JJ. Iron and infection: competition between host and microbes for a precious element. Best practice & research. Clinical haematology. 2002; 15:411–426. [PubMed: 12401315]

Nemeth E, Rivera S, Gabayan V, Keller C, Taudorf S, Pedersen BK, Ganz T. IL-6 mediates hypoferremia of inflammation by inducing the synthesis of the iron regulatory hormone hepcidin. The Journal of clinical investigation. 2004a; 113:1271–1276. [PubMed: 15124018]

Nemeth E, Tuttle MS, Powelson J, Vaughn MB, Donovan A, Ward DM, Ganz T, Kaplan J. Hepcidin regulates cellular iron efflux by binding to ferroportin and inducing its internalization. Science. 2004b; 306:2090–2093. [PubMed: 15514116]

Oexle H, Kaser A, Most J, Bellmann-Weiler R, Werner ER, Werner-Felmayer G, Weiss G. Pathways for the regulation of interferon-gamma-inducible genes by iron in human monocytic cells. Journal of leukocyte biology. 2003; 74:287–294. [PubMed: 12885946]

Pan CY, Lee SC, Rajanbabu V, Lin CH, Chen JY. Insights into the antibacterial and immunomodulatory functions of tilapia hepcidin (TH)2–3 against Vibrio vulnificus infection in mice. Developmental and comparative immunology. 2012; 36:166–173. [PubMed: 21756935]

Park CH, Valore EV, Waring AJ, Ganz T. Hepcidin, a urinary antimicrobial peptide synthesized in the liver. The Journal of biological chemistry. 2001; 276:7806–7810. [PubMed: 11113131]

Preza GC, Ruchala P, Pinon R, Ramos E, Qiao B, Peralta MA, Sharma S, Waring A, Ganz T, Nemeth E. Minihepcidins are rationally designed small peptides that mimic hepcidin activity in mice and may be useful for the treatment of iron overload. Journal of Clinical Investigation. 2011; 121:4880–4888. [PubMed: 22045566]

Ramos E, Ruchala P, Goodnough JB, Kautz L, Preza GC, Nemeth E, Ganz T. Minihepcidins prevent iron overload in a hepcidin-deficient mouse model of severe hemochromatosis. Blood. 2012; 120:3829–3836. [PubMed: 22990014]

Rodriguez R, Jung CL, Gabayan V, Deng JC, Ganz T, Nemeth E, Bulut Y, Roy CR. Hepcidin induction by pathogens and pathogen-derived molecules is strongly dependent on interleukin-6. Infection and immunity. 2014; 82:745–752. [PubMed: 24478088]

Schaible UE, Kaufmann SH. Iron and microbial infection. Nature reviews Microbiology. 2004; 2:946–953.

Shan J, Shen J, Liu L, Xia F, Xu C, Duan G, Xu Y, Ma Q, Yang Z, Zhang Q, et al. Nanog regulates self-renewal of cancer stem cells through the insulin-like growth factor pathway in human hepatocellular carcinoma. Hepatology. 2012; 56:1004–1014. [PubMed: 22473773]

Starks AM, Bourdage KL, Thiaville PC, Gulig PA. Use of a marker plasmid to examine differential rates of growth and death between clinical and environmental strains of Vibrio vulnificus in experimentally infected mice. Molecular microbiology. 2006; 61:310–323. [PubMed: 16856938]

Starks AM, Schoeb TR, Tamplin ML, Parveen S, Doyle TJ, Bomeisl PE, Escudero GM, Gulig PA. Pathogenesis of infection by clinical and environmental strains of Vibrio vulnificus in iron-dextran-treated mice. Infection and immunity. 2000; 68:5785–5793. [PubMed: 10992486]

Verga Falzacappa MV, Vujic Spasic M, Kessler R, Stolte J, Hentze MW, Muckenthaler MU. STAT3 mediates hepatic hepcidin expression and its inflammatory stimulation. Blood. 2007; 109:353–358. [PubMed: 16946298]

Waalen J, Felitti V, Gelbart T, Ho NJ, Beutler E. Prevalence of hemochromatosis-related symptoms among individuals with mutations in the HFE gene. Mayo Clinic proceedings. 2002; 77:522–530. [PubMed: 12059121]

Wallace DF, McDonald CJ, Ostini L, Subramaniam VN. Blunted hepcidin response to inflammation in the absence of Hfe and transferrin receptor 2. Blood. 2011; 117:2960–2966. [PubMed: 21245482]

Wang L, Harrington L, Trebicka E, Shi HN, Kagan JC, Hong CC, Lin HY, Babitt JL, Cherayil BJ. Selective modulation of TLR4-activated inflammatory responses by altered iron homeostasis in mice. The Journal of clinical investigation. 2009; 119:3322–3328. [PubMed: 19809161]

Webster AC, Litwin CM. Cloning and characterization of vuuA, a gene encoding the Vibrio vulnificus ferric vulnibactin receptor. Infection and immunity. 2000; 68:526–534. [PubMed: 10639413]

Weinberg ED. Iron out-of-balance: a risk factor for acute and chronic diseases. Hemoglobin. 2008; 32:117–122. [PubMed: 18274989]

Weinberg ED. Iron availability and infection. Biochimica et biophysica acta. 2009; 1790:600–605. [PubMed: 18675317]

Wright AC, Simpson LM, Oliver JD. Role of iron in the pathogenesis of Vibrio vulnificus infections. Infection and immunity. 1981; 34:503–507. [PubMed: 7309236]

Wrighting DM, Andrews NC. Interleukin-6 induces hepcidin expression through STAT3. Blood. 2006; 108:3204–3209. [PubMed: 16835372]

Zoller H, Theurl I, Koch R, Kaser A, Weiss G. Mechanisms of iron mediated regulation of the duodenal iron transporters divalent metal transporter 1 and ferroportin 1. Blood cells, molecules & diseases. 2002; 29:488–497.

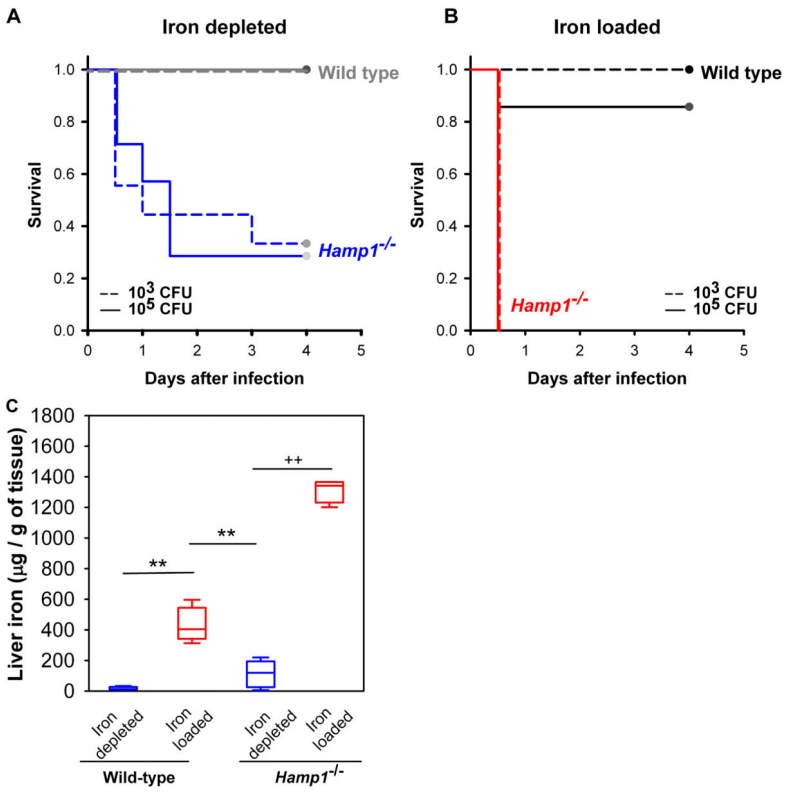

Figure 1. *Vibrio vulnificus* infection is highly lethal in hepcidin-deficient mice

Kaplan-Meier survival curves for iron depleted **(A)** and iron loaded **(B)** mice, after infection with $1x10^3$ (dashed lines) or $1x10^5$ (solid lines) CFU of *V. vulnificus* (n=4–11 in each group). WT and *Hamp1*$^{-/-}$ mice were iron-depleted or iron-loaded by dietary modification (WT: 4 ppm or 10,000 ppm Fe diet for 2 weeks; *Hamp1*$^{-/-}$: 4 ppm or standard diet for 4–6 weeks, see Methods). By multifactorial Kaplan-Meier Log-Rank analysis, differences in survival between WT and *Hamp1* $^{-/-}$ mice were significant in both iron depleted (combined CFU, $p<0.05$), and iron-loaded conditions (combined CFU, $p<0.001$). **(C)** Liver iron stores were measured in a parallel set of mice and confirmed the effective modulation of iron stores by dietary iron manipulation (n=5–10 per group). For liver iron measurements, statistical significance was assessed using student's *t* test if data were normally distributed (**$p<0.01$) or Mann-Whitney *U* test if they were not normally distributed ($^{++}p<0.01$). See also Figure S1.

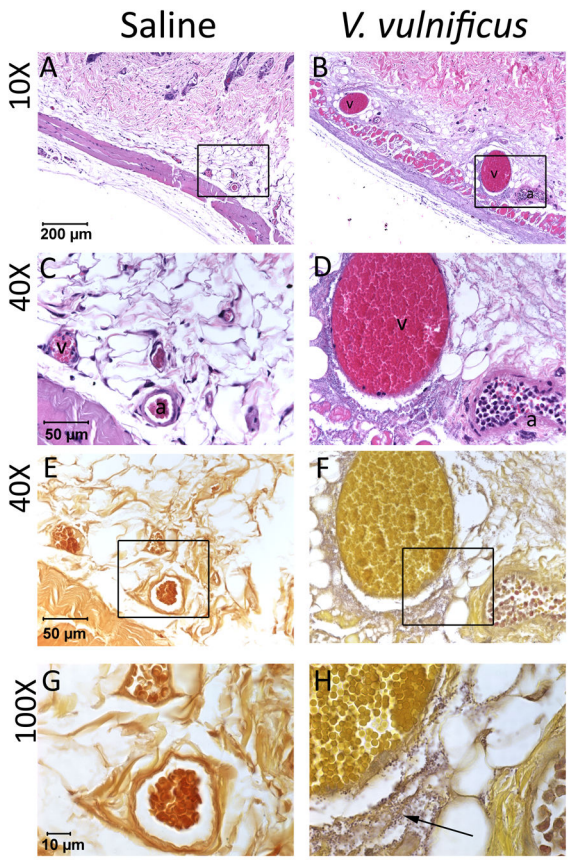

Figure 2. Local *V. vulnificus* proliferation induces vasodilation, leukostasis and erythrocyte sludging

Skin sections at the site of injection with saline (A, C, E and G) or 1 x 10^3 CFU of *V. vulnificus* (B, D, F, H) in *Hamp1*$^{-/-}$ mice. Sections were stained with hematoxylin and eosin (A–D) or Gram stain and tartrazine (E–H). **Panels A–B** and magnified in **C–D:** Dilated venules (v) and arterioles (a), leukostasis and erythrocyte sludging are seen in the skin of *V. vulnificus*-infected mice compared with saline-injected controls**. Panels E–F** and magnified in **G–H:** Numerous bacteria (purple) are seen in perivascular spaces of infected mice (arrow). See also figure S2.

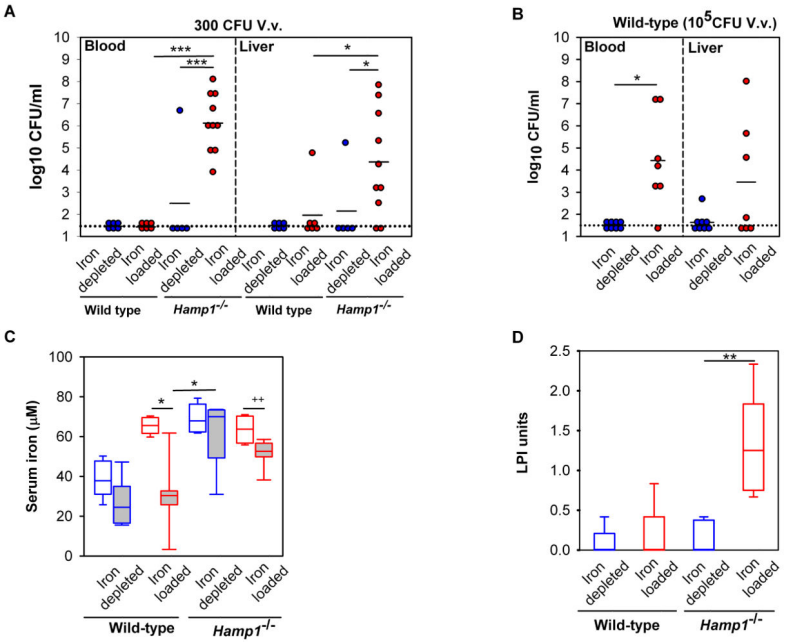

Figure 3. Iron-dependent dissemination of *V. vulnificus* in blood and liver

Wild-type and *Hamp1*$^{-/-}$ mice were iron-depleted or iron-loaded by dietary modification (WT: 4 ppm or 10,000 ppm Fe diet for 2 weeks; *Hamp1*$^{-/-}$: 4 ppm or standard diet for 4–6 weeks, see Methods), and infected with *V. vulnificus* (n=5–10 per group). **(A)** and **(B)** Bacterial counts in blood and liver 16 h after infection with 300 CFU (A) and 1x10^{5}CFU (B). Each symbol represents one mouse (iron depleted in blue and iron loaded in red); black solid lines represent the mean of CFU counts; black dotted line represents the lower limit of detection of CFU counts (calculated as half of the minimum detectable CFU counts). **(C)** Serum iron levels of WT (1x10^{5}CFU) and *Hamp1*$^{-/-}$(300 CFU) mice (white fill = saline groups, grey fill = *V. vulnificus* groups). Unlike WT mice which decreased their serum iron to the mean of ~30 μM, *Hamp1*$^{-/-}$ mice did not develop marked hypoferremia after infection. **(D)** Measurement of non-transferrin bound iron in serum of iron-depleted and iron-loaded WT and *Hamp1*$^{-/-}$ mice prior to infection (n=4–6 per group). Statistical significance was assessed using student's *t* test if data were normally distributed (*p<0.05; **p<0.01; ***p<0.001) or Mann-Whitney *U* test if they were not ($^{+}$p<0.05; $^{++}$p<0.01). See also Figure S3.

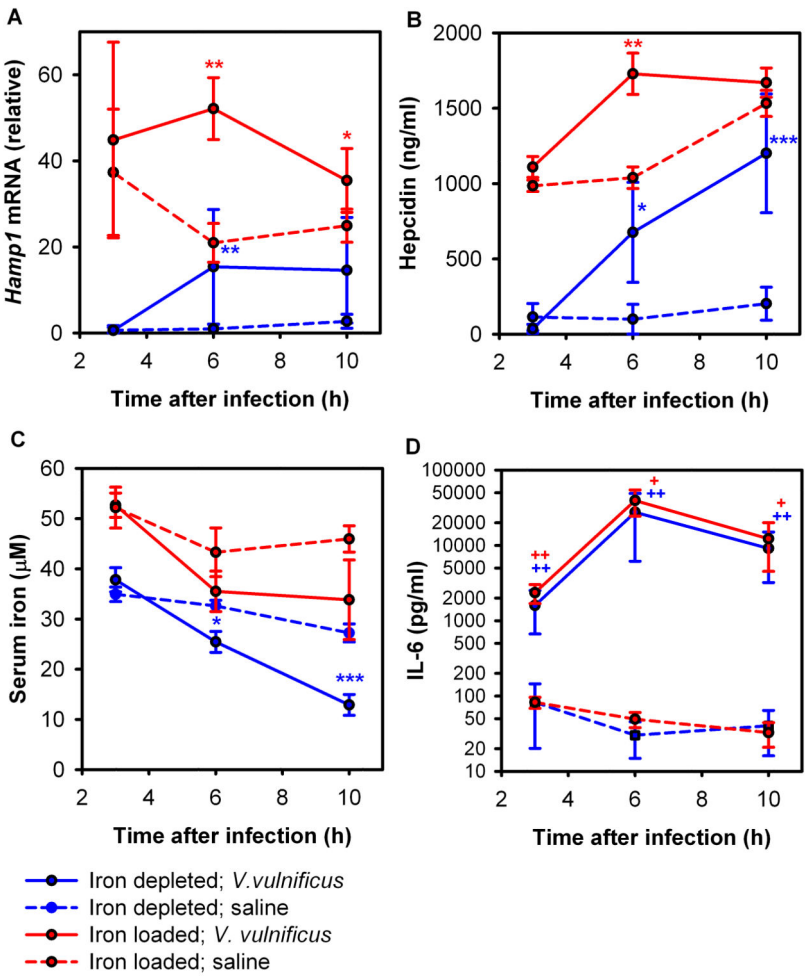

Figure 4. WT mice respond to *V. vulnificus* infection by rapidly increasing plasma hepcidin concentration

WT mice, either iron-depleted (blue) or iron-loaded (red), were injected with 10^5 CFU *V. vulnificus* (solid lines) or saline (dashed lines) and euthanized after 3, 6 or 10 hours. **(A)** Hepatic *Hamp1* mRNA expression. **(B)** Serum hepcidin concentration. **(C)** Serum iron concentration. **(D)** The inflammatory response to infection was confirmed by serum IL-6 assay. Each point represents the mean ± standard deviation (n=5). Statistical significance was assessed using student's *t* test if data were normally distributed (*p<0.05; **p<0.01; ***p<0.001) or Mann-Whitney *U* test if they were not ($^{+}$p<0.05; $^{++}$p<0.01). See also Figure S4.

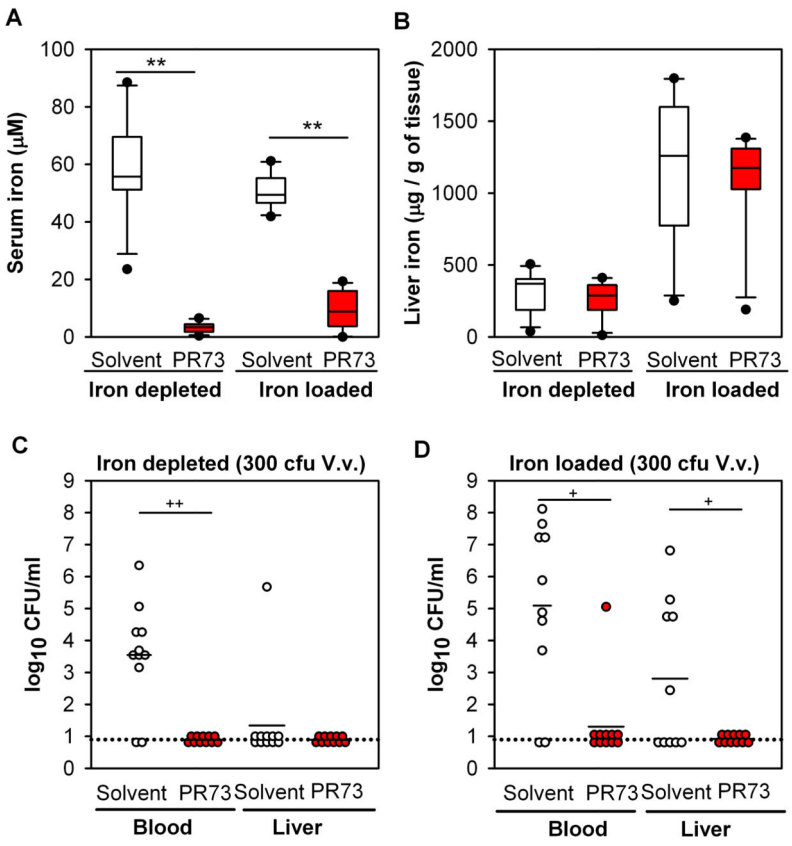

Figure 5. Minihepcidin PR73 decreases infection by *V. vulnificus* in *Hamp1*$^{-/-}$ mice

Hamp1$^{-/-}$ mice (either iron-depleted or iron-loaded) were treated with 100 nmol of PR73 (red symbols) or solvent (white symbols) 24h and 3h before infection with 300 CFU *V. vulnificus*. Mice were euthanized 16h after infection. N=10–11 per group. **(A)** Serum iron was markedly decreased in PR73-injected mice, with no difference in serum iron between solvent-injected iron-depleted and iron-loaded mice. **(B)** Liver iron was higher in iron-loaded than iron-depleted mice as expected. PR73 administration did not result in significant changes in liver iron stores. **(C)** and **(D)** *V. vulnificus* was undetectable in blood and liver in PR73-treated mice, in contrast to mice treated with saline. Each dot represents one mouse; black solid lines represent the mean of CFU counts. The black dotted line represents the lower limit of detection of CFU counts (calculated as half of the minimum detectable CFU counts). Statistical significance was assessed using student's *t* test if data were normally distributed (**p<0.01) or Mann-Whitney *U* test if they were not ($^{+}$p<0.05; $^{++}$p<0.01). See also Figure S5.

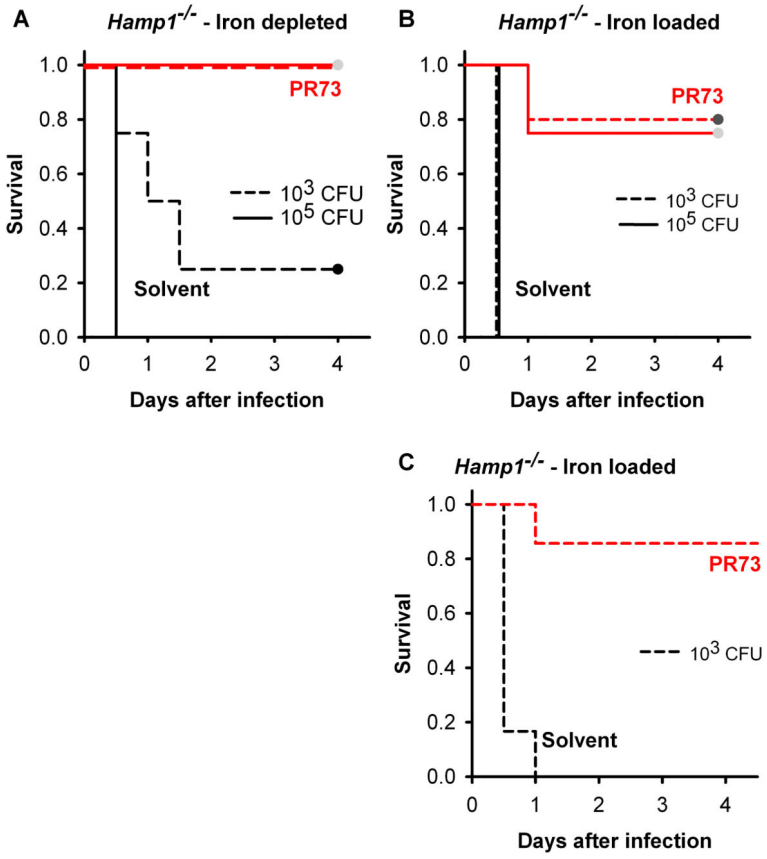

Figure 6. Minihepcidin PR73 prevents death due to *V. vulnificus* infection in *Hamp1*$^{-/-}$ mice

Kaplan-Meier survival curves, n=4–5 per group. Both iron-depleted **(A)** and iron-loaded **(B)** *Hamp1*$^{-/-}$ mice survived the infection with 10^3 and 10^5 CFU *V. vulnificus* when treated with 100 nmol PR73 (red) before the infection. **(C)** *Hamp1*$^{-/-}$ mice were resistant to infection even if PR73 was administered 3h after infection. Statistically significant differences in survival between solvent- and PR73-treated mice were assessed using the Log-Rank survival analyzes: $p<0.05$ for iron-depleted, 10^3 CFU; $p<0.01$ for the other groups. See also Figure S6.

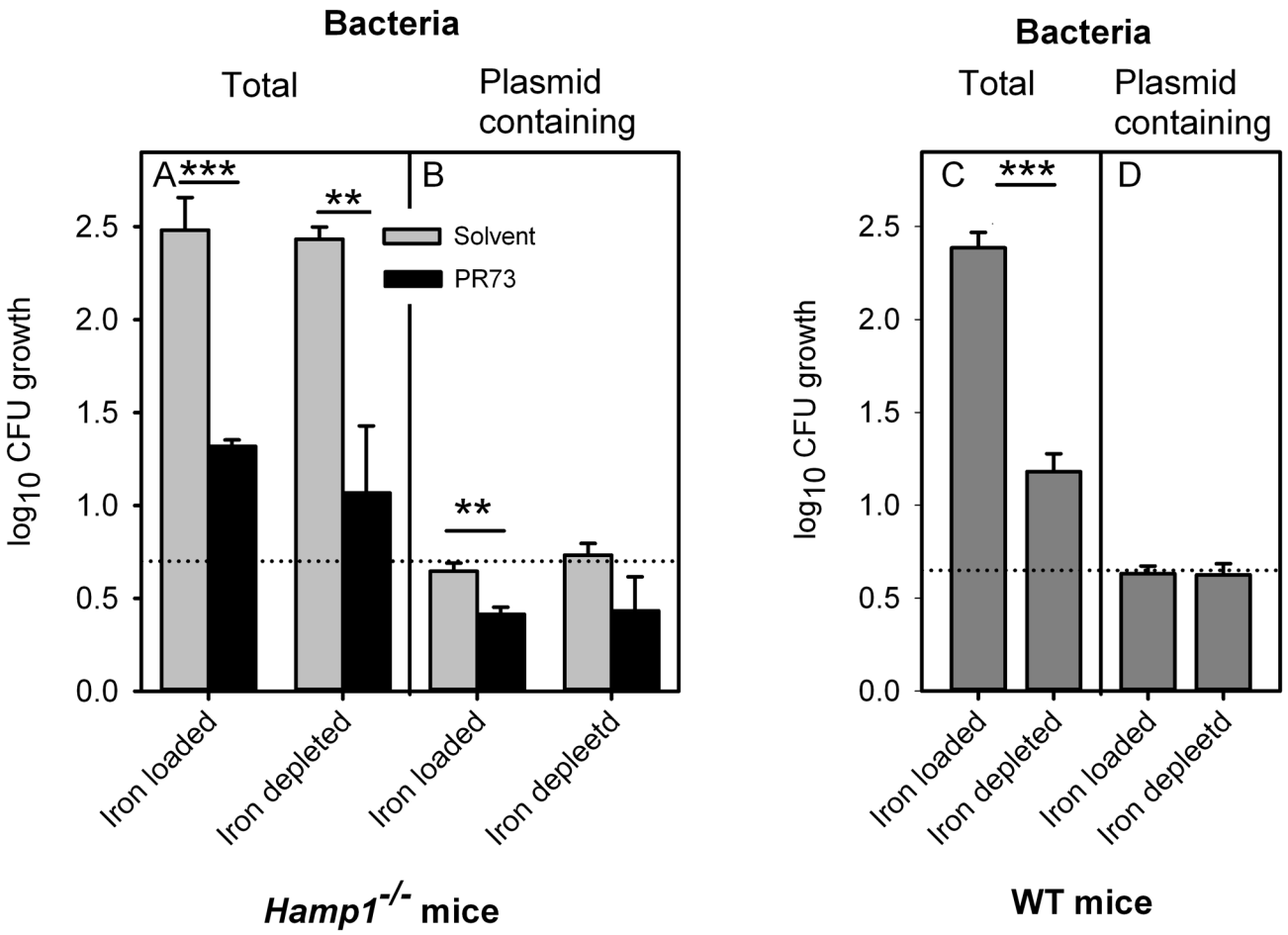

Figure 7. Minihepcidin PR73 acts in serum by slowing bacterial growth

Serum was collected from iron-depleted or iron-loaded *Hamp1*$^{-/-}$ mice that were injected with PR73 or solvent, and from iron-depleted or iron-loaded WT mice (not treated with PR73). Serum iron concentrations are shown in Table S2. *V. vulnificus* carrying the non-replicating marker plasmid pGTR905 was incubated in these sera *in vitro* for 2 h, and CFU were determined either on plates without chloramphenicol (**total** bacteria) or plates with chloramphenicol and arabinose (allows growth of only **plasmid-containing** bacteria). **(A)** PR73 greatly reduced total bacterial yield, which reflects the sum of bacteriostatic and bactericidal effects. **(B)** PR73 only slightly reduced the yield of plasmid-containing bacteria indicating only a small bactericidal effect. **(C)** The number of total bacteria was much higher in serum from iron-loaded WT mice than in serum from iron-depleted mice, as expected. **(D)** Different serum iron concentrations did not affect the yield of plasmid-containing bacteria indicating that hypoferremia by itself does not have a bactericidal effect. Each vertical bar represents the mean, and error bars represent standard deviation for 3 independent experiments (with 3 replicates in each experiment). The black dotted line represents the number of plasmid-containing bacteria after growth that diluted plasmid copy number to 1 plasmid per bacterium (thus bacteria in the original inoculum carried 5 plasmids

per bacterium). Statistical significance was assessed using student's *t* test (*p<0.05; **p<0.01; ***p<0.001). See also Figure S7.